

AFRL-ML-WP-TP-2006-437

**PERMEABILITY OF POLYMER
COMPOSITES FOR CRYOGENIC
APPLICATIONS (PREPRINT)**



Vernon T. Bechel and Fred Arnold

MARCH 2006

Approved for public release; distribution is unlimited.

STINFO COPY

This work has been submitted for publication in proceedings of the 2006 National Space and Missile Materials Symposium. This is a work of the U.S. Government and is not subject to copyright protection in the United States.

**MATERIALS AND MANUFACTURING DIRECTORATE
AIR FORCE RESEARCH LABORATORY
AIR FORCE MATERIEL COMMAND
WRIGHT-PATTERSON AIR FORCE BASE, OH 45433-7750**

REPORT DOCUMENTATION PAGE				Form Approved OMB No. 0704-0188	
<p>The public reporting burden for this collection of information is estimated to average 1 hour per response, including the time for reviewing instructions, searching existing data sources, gathering and maintaining the data needed, and completing and reviewing the collection of information. Send comments regarding this burden estimate or any other aspect of this collection of information, including suggestions for reducing this burden, to Department of Defense, Washington Headquarters Services, Directorate for Information Operations and Reports (0704-0188), 1215 Jefferson Davis Highway, Suite 1204, Arlington, VA 22202-4302. Respondents should be aware that notwithstanding any other provision of law, no person shall be subject to any penalty for failing to comply with a collection of information if it does not display a currently valid OMB control number. PLEASE DO NOT RETURN YOUR FORM TO THE ABOVE ADDRESS.</p>					
1. REPORT DATE (DD-MM-YY) March 2006		2. REPORT TYPE Conference Paper Preprint		3. DATES COVERED (From - To)	
4. TITLE AND SUBTITLE PERMEABILITY OF POLYMER COMPOSITES FOR CRYOGENIC APPLICATIONS (PREPRINT)				5a. CONTRACT NUMBER In-house	
				5b. GRANT NUMBER	
				5c. PROGRAM ELEMENT NUMBER N/A	
6. AUTHOR(S) Vernon T. Bechel and Fred Arnold				5d. PROJECT NUMBER N/A	
				5e. TASK NUMBER N/A	
				5f. WORK UNIT NUMBER N/A	
7. PERFORMING ORGANIZATION NAME(S) AND ADDRESS(ES) Structural Materials Branch (AFRL/MLBC) Nonmetallic Materials Division Materials and Manufacturing Directorate Air Force Research Laboratory, Air Force Materiel Command Wright-Patterson Air Force Base, OH 45433-7750				8. PERFORMING ORGANIZATION REPORT NUMBER AFRL-ML-WP-TP-2006-437	
9. SPONSORING/MONITORING AGENCY NAME(S) AND ADDRESS(ES) Materials and Manufacturing Directorate Air Force Research Laboratory Air Force Materiel Command Wright-Patterson AFB, OH 45433-7750				10. SPONSORING/MONITORING AGENCY ACRONYM(S) AFRL-ML-WP	
				11. SPONSORING/MONITORING AGENCY REPORT NUMBER(S) AFRL-ML-WP-TP-2006-437	
12. DISTRIBUTION/AVAILABILITY STATEMENT Approved for public release; distribution is unlimited.					
13. SUPPLEMENTARY NOTES This work has been submitted for publication in proceedings of the 2006 National Space and Missile Materials Symposium. This is a work of the U.S. Government and is not subject to copyright protection in the United States. This paper contains color. PAO Case Number: AFRL/WS 06-0852, 03 Apr 2006.					
14. ABSTRACT Previous cryogenic cycling research has focused on improving our understanding of the mechanisms that lead to a leakage-producing network of cracks in carbon/epoxy and carbon/bismaleimide composites and to evaluate a number of materials for use in cryogenic pressure vessels. However, the large fuel tanks and other cryogenic components of future reusable launch vehicles may benefit from the use of even higher temperature composite materials through the reduction in the weight of the thermal protection system needed to protect the composite components inside the vehicle. Hence, the current effort investigated two carbon/polymer composites (T650/AFR-PE-4 and T650/BIM-15) with service temperatures considerable greater than for most carbon/epoxy and carbon/bismaelimide composites. Additionally, to determine the effect of a more destructive thermal cycle, T650/AFR-PE-4 samples were also subjected to thermal cycling that included an elevated hold of 315 °C.					
15. SUBJECT TERMS Carbon/epoxy, carbon bismaleimide, T650/AFR-PE-4, T650/BIM-15, temperature					
16. SECURITY CLASSIFICATION OF:			17. LIMITATION OF ABSTRACT: SAR	18. NUMBER OF PAGES 18	19a. NAME OF RESPONSIBLE PERSON (Monitor) Vernon T. Bechel 19b. TELEPHONE NUMBER (Include Area Code) N/A
a. REPORT Unclassified	b. ABSTRACT Unclassified	c. THIS PAGE Unclassified			

Permeability of Polymer Composites for Cryogenic Applications

Vernon T. Bechel* and Fred Arnold*

Air Force Research Laboratory, Wright Patterson AFB, OH 45433

Previous cryogenic cycling research has focused on improving our understanding of the mechanisms that lead to a leakage-producing network of cracks in carbon / epoxy and carbon / bismaleimide composites and to evaluate a number of materials for use in cryogenic pressure vessels. However, the large fuel tanks and other cryogenic components of future reusable launch vehicles may benefit from the use of even higher temperature composite materials through the reduction in the weight of the thermal protection system needed to protect the composite components inside the vehicle. Hence, the current effort investigated two carbon / polymer composites (T650 / AFR-PE-4 and T650 / BIM-15) with service temperatures considerably greater than for most carbon / epoxy and carbon / bismaleimide composites. Following cryogenic cycling of these “high temperature PMCs”, the ply-by-ply micro-crack densities and resulting permeabilities were compared to the corresponding data from IM7 / 5250-4 carbon / bismaleimide composite. After 1250 cycles from -196 °C to 177 °C the helium permeability of IM7 / 5250-4 [0/45/-45/90]_s at room temperature was approximately 5×10^{-5} scc/s-cm², but only 250 cycles were needed to reach a similar permeability for the T650 / AFR-PE-4 samples. Additionally, to determine the effect of a more destructive thermal cycle, T650 / AFR-PE-4 samples were also subjected to thermal cycling that included an elevated hold of 315 °C.

I. Introduction

The conventional launch vehicles and / or hypersonic air/spacecraft that will replace the Space Shuttle and are intended to be reusable for hundreds of missions will likely incorporate large pressure vessels for cryogenic liquids such as liquid oxygen or liquid hydrogen. Polymer matrix composites (PMC) have been investigated for several years as lightweight structural materials that would have beneficial application in these tanks.¹⁻² During the course of these investigations a number of research efforts have looked at the fundamental problem of how best to choose or design a composite that will remain leak free (despite containing layers with varying thermal expansion characteristics) throughout the life of vehicle that is being filled and flown multiple times.³⁻⁶ A common theme of the experimental efforts has been to subject a composite to a number of mechanical and / or thermal cycles that may include both cryogenic and elevated temperature holds. In this way, the temperatures experienced during fill, launch, and re-entry are simulated. One of several parameters shown to be critical to the damage development and leakage resistance of a composite is the elevated temperature applied during combined cryogenic and elevated temperature cycling. It has been shown for some of the aerospace grade carbon / epoxy and carbon / bismaleimide composites that when a greater temperature is used for the elevated temperature hold, significantly increased permeability results in fewer thermal cycles.⁷

Recently engineers conceptualizing designs of reusable space vehicles have begun to seriously consider using higher temperature PMCs. The motivation for using these materials is that if a PMC with a greater service temperature is used, the interior of the vehicle can be allowed to reach a greater peak temperature during or after re-entry as the heat generated at the vehicle surface during re-entry is thermally conducted (“soaked”) into the vehicle interior. However, these high temperature PMCs have a number of disadvantages that the “medium temperature” epoxies and bismaleimides often do not. First, the matrix in the high temperature PMC has been designed for high temperature performance rather than low temperature performance, and therefore, is unlikely to have been formulated with adequate low-temperature toughness as a desired property. Second, high temperature PMCs are commonly cured at much greater temperatures. This greater cure temperature results in more substantial residual stresses at ambient and low temperature conditions. Consequently, the transverse tensile stress in some or all of the

* Materials Research Engineer, Structural Materials Branch, AFRL/MLBC

plies will be greater in the high temperature material at low temperature as compared to the medium temperature material (all other parameters being equal). Finally, if allowed to reach a greater peak temperature in service, the high temperature material would be subject to a more damaging thermal cycle. The difference between the upper and lower temperature during thermal fatigue would be greater. As in mechanical fatigue of composites, if the difference in stress between the loaded and the unloaded state is increased, greater amounts of damage occur and the fatigue life may be reduced.⁹ Further, as already stated, previous work in this area has already indicated that a higher temperature during combined cryogenic and elevated temperature cycling produces more damage and permeability^{7,8} in a number of the composites that have been tested to date. As a result, the pattern of damage development due to cryogenic cycling needs to be studied in these materials.

Previous cryogenic cycling research has been conducted to measure the extent of damage generated in carbon / epoxy and carbon / bismaleimide matrix composites such as IM7 / 977-2 and IM7 / 5250-4. In addition, several papers describe experimental work to relate this damage to the resulting permeability of the materials. On the other hand, the published research on cryogenic testing of high temperature PMCs with, for example, a service temperature of 232 °C or greater is limited.^{8,10} Ju, *et.al*, conducted combined cryogenic temperature (-196 °C), elevated temperature (up to 250 °C), and mechanical cycling on M40J / PMR-II-50 and concluded, among other things, that the strength of the fiber / matrix interface in this high temperature carbon / polyimide composite was degraded by the applied thermal cycling.⁸ The current effort investigated two carbon / polyimide composites - T650 / AFR-PE-4 and T650 / BIM-15 - both with service temperatures considerably greater than for bismaleimide composites. Following cryogenic cycling of these PMCs (-196 °C to 177 °C), the ply-by-ply micro-crack densities and resulting permeability were compared to the corresponding data from a baseline carbon / bismaleimide composite - IM7 / 5250-4. Also, to determine if T650 / AFR-PE-4 was susceptible to additional damage development as a function of increasing temperature in the elevated portion of the thermal cycle, a second set of T650 / AFR-PE-4 samples was subjected to 250 cycles that consisted of cycling between liquid nitrogen temperature (-196 °C) and 315 °C.

II. Experimental

A. Materials

Two carbon / polyimide composites with a maximum continuous dry service temperature that places them in the category of high temperature PMCs (service temperature beyond 232 °C) were pre-conditioned and tested for permeability. They were chosen because they are representative of high temperature, high performance structural composites used in the aerospace industry. The fibers in each composite were intermediate modulus T650 carbon fibers from Cytec. The first composite had a 315 °C maximum service temperature addition polyimide matrix, AFR-PE-4, from Maverick. The second material had a 232 °C maximum service temperature (possibly as high as 288 °C for non-aircraft applications) addition polyimide matrix, BIM-15, from Maverick. The results from these two materials were compared to the results for a third (baseline) material, IM7 / 5250-4, which consisted of medium modulus IM7 fibers from Hexcel and a 204 °C maximum service temperature bismaleimide matrix from Cytec. [0/+45/-45/90]_s laminates of the T650 / AFR-PE-4 and IM7 / 5250-4 and [0/90]_{2s} laminates of the T650 / BIM-15 and IM7 / 5250-4 were hand laid-up and autoclave cured. The laminates of all three materials had a single ply thickness of 0.13 to 0.14 mm. 50 mm by 50 mm square samples were cut from the cured panels with the 0° plies parallel to one side of each sample.

B. Cryogenic Cycling / Damage Measurement

The thermal cycling apparatus consisted of a frame and stepper motor actuation system that moved a wire mesh sample container between positions inside a dewar of liquid nitrogen (LN₂), in front of an ambient air fan, and inside an oven (Figure 1). A solenoid valve electrically controlled by a silicon transistor temperature sensor, maintained the LN₂ level in the dewar. A 46 cm tall custom-made 1000 W convection oven above the ambient air fan provided the elevated portion of the thermal cycle. The bottom of the oven contained a 16 cm circular opening for the sample container to pass through. As with the top of the LN₂ dewar, the bottom of the oven remained open during cycling. Based on measurements of temperature equilibration times in samples with an embedded thermocouple, a cycle of 2 minutes in the LN₂ followed by 5 minutes at room temperature and 5 minutes in the oven was used. Each sample was polished on perpendicular sides prior to cycling, and ply-level cracks were observed on the sample edges at 200X with an optical microscope after 0, 1, 5, 15, 30, 75, 125, 175, and 250 cycles. The T650 / BIM-15 samples were further observed for cracks after 325, 400, 500, and 750 cycles. Cracks were counted along the full length of each edge. Only transverse cracks that extended fully through the thickness of a ply (or nearly through the

thickness) were counted. Crack densities were recorded on each side for all plies for which fiber ends (and thus transverse cracks) were visible. The side with the fiber *ends* visible on the 0° plies will be referred to as Side A, and correspondingly, Side B was the side with the fiber *sides* visible on the 0° plies. The crack densities from four samples of each laminate were averaged. Additionally, the crack densities in the $\pm 45^\circ$ plies were scaled by dividing the cracks density by $\sin(45^\circ)$.

C. Permeability Apparatus and Testing Parameters

The permeability apparatus is shown in Figure 2. A differential pressure was created across the sample to potentially create a flow of gas through the sample thickness and into a control volume. If the sample had one or more complete chains of micro-cracks extending through the sample thickness, measurable flow would occur. The gas flow rate was determined by measuring the increase in pressure in the control volume as a function of time. The rate of pressure change was then converted to a flow rate using the ideal gas law. The apparatus had two independent vacuum systems. The vacuum chamber on the left in Figure 2 is the control volume for determining the flow through the sample, and the smaller vacuum chamber on the right provided vacuum for a mass spectrometer. These two chambers were connected on occasion with a precision leak valve to transfer a gas sample from the control volume to the mass spectrometer which was used to verify that helium was flowing through the sample. The pressure in the control volume was monitored with a Baratron-type transducer with a resolution of 1×10^{-3} torr.

The sample was sealed between two small “sample chambers” each consisting of an NW25 Kwik flange and a Viton o-ring to seal them to the sample. The upstream chamber was used to apply helium gas at 0.28 MPa (40 psi) to one side of the sample, and the downstream chamber was used to maintain a vacuum on the other side of the sample to allow a medium resolution measurement of pressure. All of the permeability tests were conducted at ambient temperature. Cracks in the surface plies were observed in all samples after less than 75 thermal cycles. These cracks provided a path for ambient air to bypass the seal on the measurement side of the sample and flow into the sample chamber and control volume. This “background flow” was measured for each sample prior to running a permeability test so that it could be separated from the flow of helium through the sample once the supply side was pressurized. In previous work⁷ indium gaskets and an epoxy sealant on the surface of the samples were used to prevent flow through the surface cracks. However, applying the indium gasket and epoxy sealant altered the sample sufficiently that it could not be further cycled. I.e., a new set of samples had to be made and cycled further than the previous set of samples. Hence, in this project a compromise approach was chosen. The Viton o-ring was used to seal the samples chambers to the sample. As already mentioned, this method of sealing did not prevent flow through the surface ply cracks, but it left the sample unaltered by permeability testing – allowing the same set of samples for a given material to be used for all increments of cycling. On the other hand, the flow rate of air through surface cracks was typically high compared to the small helium flow rates through the sample thickness that were common when complete leak paths through the material *initially formed*. Since these initial through-thickness flows were close to the resolution of the experiment, they could not accurately be separated from the background air flow through the surface ply cracks. Therefore, permeability measurements were not reported until they reached approximately 1×10^{-7} scc / s-cm². Note: the exception to this is the permeability data reported for IM7 / 5250-4 which is taken from reference 7. While in previous work⁷ permeabilities were reported as low as 1×10^{-9} scc /s-cm², the important trends in permeability versus number of cycles were observable with the current approach. This compromise allowed much quicker and more practical testing to be accomplished since fewer samples needed to be cycled and scanned to count cracks.

Permeability was measured at room temperature after 125, 175, and 250 cycles of the combined cryogenic and elevated temperature thermal cycles for the T650 / AFR-PE-4 [0/45/-45/90]_S samples and after 500 and 750 cycles for the T650 / BIM-15 [0/90]_{2S} samples. Four samples were tested after each increment of cycling. The test length ranged from 100 seconds to 400 seconds depending on whether the helium flow was high or low compared to the background flow. A 0.001 torr pressure increase in the 14 liter control volume measured over an interval of 400 seconds represented a flow of 5.75×10^{-9} scc/s-cm² of helium through the 7.29 cm² flow area of the sample and thus, established the best possible resolution of the permeability measurement. However, as previously discussed, it was commonly not possible to accurately separate the background flow from the through-thickness flow for through-thickness flow rates below 1.15×10^{-7} scc/s-cm². Note, “permeability” as used in this context is defined as the flow rate of a particular gas through a material under a prescribed set of boundary conditions.

III. Results

A. T650 / AFR-PE-4 Permeability

[0/45/-45/90]_s samples of IM7 / 5250-4 and T650 / AFR-PE-4 with equal ply thickness were cycled with the same -196 °C to 177 °C thermal cycle so a direct comparison of their permeability and damage state could be made. As shown in Figure 3, the T650 / AFR-PE-4 samples developed substantial permeability much quicker than the IM7 / 5250-4 samples. After 1250 of the -196 °C to 177 °C cycles the helium permeability of the IM7 / 5250-4 samples at room temperature was approximately 5×10^{-5} scc/s-cm² while only 250 cycles were needed to reach a similar permeability for the T650 / AFR-PE-4 samples. Also, the permeability as a function of thermal cycles was not tending to saturation (leveling off) by 250 cycles. Consequently, greater permeabilities would be expected in both materials with further cycling. This trend is especially a concern for the T650 / AFR-PE-4 samples since the permeability is increasing at a much higher rate of nearly an order of magnitude for each 75 cycles applied.

A separate set of four samples of the same [0/45/-45/90]_s panel of T650 / AFR-PE-4 were cycled from -196 °C to the 315 °C service temperature of AFR-PE-4. The permeability results as a function of cycles are shown in Figure 4 along with a plot of the permeability of the T650 / AFR-PE-4 samples cycled from -196 °C to 177 °C. Surprisingly, the permeabilities of the samples cycled from -196 °C to 315 °C are lower after 125 cycles, nearly the same after 175 cycles and greater after 250 cycles. No clear trend is apparent. However, when considered in the context of past research,⁷ AFR-PE-4 did not exhibit nearly the sensitivity to an increase in elevated hold temperature as, for example, IM7 / 5250-4 or IM7 / 977-3 (carbon / epoxy) composites. The permeability of samples these materials with the same [0/45/-45/90]_s lay-up increased as much as 20 times for an increase in the elevated hold temperature of only 55 °C while the permeability of the AFR-PE-4 samples increased by a maximum of only 5 times for an increase in the elevated hold temperature of 138 °C.

B. T650 / AFR-PE-4 Damage Accumulation

Figure 5 shows the micro-crack densities in each ply of the T650 / AFR-PE-4 [0/45/-45/90]_s samples that were cycled between -196 °C and 177 °C and Figure 6 shows the same type of micro-crack density data for the IM7 / 5250-4 samples of the same lay-up cycled with the same thermal cycle. The IM7 / 5250-4 samples developed greater micro-crack densities in the surface plies after fewer cycles – almost two times greater after 250 cycles. However, the T650 / AFR-PE-4 samples overall had greater micro-crack densities in the inner plies, especially in plies 3 and 6 which remained un-cracked in the IM7 / 5250-4 samples through 175 cycles and had only 0.10 micro-crack / cm after 250 cycles. Compare this to the T650 / AFR-PE-4 samples that had greater than 1.8 cracks / cm in all plies after 250 cycles. For significant permeability to occur, complete paths consisting of connected micro-cracks are more important than the number of cracks in any individual ply. Therefore, the greater tendency for substantial crack densities *in all plies* of the T650 / AFR-PE-4 is consistent with the greater measured permeability through 250 cycles.

The pattern of crack propagation in the T650 / AFR-PE-4 is similar to the pattern observed in IM7 / 5250-4 in several respects. Cracks in plies 2 and 7 were always within a ply thickness in the horizontal direction of the ply 1 and 8 cracks indicating that they propagated from plies 1 and 8 into plies 2 and 7 as stitch cracks. The term “stitch crack” refers to a crack fully through the ply thickness but relatively short in the planar direction that is centered on a long parent crack in an adjacent ply and propagates from the parent crack. This pattern of crack propagation has been discussed extensively in previous work and was also observed in IM7 / 5250-4. The same order of crack growth from plies 4 and 5 into plies 3 and 6 as stitch cracks was observed in both materials. However, one important difference is shown in Figure 7. In the T650 / AFR-PE-4 samples large delaminations formed between the +45° and -45° plies and in some cases between the other plies after as few as 175 cycles. While small delaminations were observed in the IM7 / 5250-4 between various plies where stitch cracks were being extended into a neighboring ply, no delaminations were observed between the +45° and -45° plies. The large delaminations between the +45° and -45° plies in the T650 / AFR-PE-4 samples likely aided significantly in completing leakage paths by providing the final link between the stitch cracks in the +45° and -45° plies.

Figure 8 shows the micro-crack densities in each ply of the T650 / AFR-PE-4 [0/45/-45/90]_s samples that were cycled between -196 °C and 315 °C. All plies of the samples had much greater crack densities than for the T650 / AFR-PE-4 samples that were cycled between -196 °C and 177 °C. With the exception of the surface plies, approximately twice as many cracks formed after 250 cycles when cycled between -196 °C and 315 °C as compared to the results from cycling between -196 °C and 177 °C (Figure 5). The greater crack densities are consistent with the greater permeability after 250 cycles as shown in Figure 4, but not with the lower permeability at 125 cycles.

C. T650 / BIM-15 Permeability

The permeability of the T650 / BIM-15 [0/90]_{2S} samples was measured after 500 and 750 of the -196 °C to 177 °C cycles. Many more cycles were required for the T650 / BIM-15 samples to reach a permeability of 1×10^{-7} scc/s-cm² than for the T650 / AFR-PE-4 [0/45/-45/90]_S samples. This delay before substantial permeability does not necessarily indicate that T650 / BIM-15 is a more leak resistant material than T650 / AFR-PE. Bechel, *et al.*^{4,7} showed for IM7 / 5250-4 that samples of a [0/90]_{2S} lay-up were more leak resistant than samples of a [0/45/-45/90]_S lay-up of the same material when thermally cycled with the same cycle. Consequently, the results for the T650 / BIM-15 cannot be compared to the results for T650 / AFR-PE-4 since different lay-ups were used. Note: The next step in this project will be to test a [0/90]_{2S} lay-up of the AFR-PE-4 composite.

The permeability results for T650 / BIM-15 are shown in Figure 9 along with the permeability of the IM7 / 5250-4 [0/90]_{2S} samples through 1500 of the -196 °C to 177 °C cycles. While the IM7 / 5250-4 samples exhibited no measurable permeability ($<1 \times 10^{-9}$ scc/s-cm²) through 1500 cycles, the T650 / BIM-15 samples had permeability at least 15 times greater by 500 cycles and three orders of magnitude greater by 750 cycles. Clearly, the high temperature material PMC (T650/BIM-15) was much less resistant to combined cryogenic and elevated temperature cycling than the medium temperature PMC (IM7/5250-4) even when cycled with the same medium temperature thermal cycle.

IV. Conclusions

Both high temperature PMCs (T650 / AFR-PE-4 [0/45/-45/90]_S and T650 / BIM-15 [0/90]_{2S}) had greater permeability following thermal cycling when compared with IM7 / 5250-4 samples of the corresponding lay-up. In the most extreme case, the T650 / AFR-PE-4 [0/45/-45/90]_S samples reached a permeability of 5×10^{-5} scc/s-cm² 1000 cycles sooner than the IM7 / 5250-4 samples when cycled between -196 °C and 177 °C. Similarly, the T650 / BIM-15 cross-ply samples had a measurable permeability of 1×10^{-6} scc/s-cm² after 750 cycles while the corresponding samples of IM7 / 5250-4 had no measurable permeability ($<10^{-9}$ scc/s-cm²) through 1500.

The total number of cracks in all plies of the T650 / AFR-PE-4 [0/45/-45/90]_S was similar to the total number of cracks in the IM7 / 5250-4 samples. However, the T650 / AFR-PE-4 samples had a more uniform distribution of cracks from ply to ply resulting in *many cracks in all plies*. IM7 / 5250-4, on the other hand, had larger numbers of cracks in the surface plies but lower numbers of cracks in the internal plies, with almost none in two of the plies. The more uniform pattern of cracking with respect to plies and the development of large delaminations in the T650 / AFR-PE-4 samples are believed to have resulted in a greater number of complete leakage paths through the material and consequently, are the likely source of the greater permeability. These trends indicate that implementing high temperature PMCs in cryogenic components of reusable launch vehicles to reduce TPS requirements will most likely require more careful material, lay-up, and service temperature profile considerations than those for implementing medium temperature PMCs.

Acknowledgements

The authors would like to thank Ron Trejo (UDRI) for help with composite panel fabrication.

References

1. Achary, D.C., Biggs, C.G., Bouvier, C.G., McBain, M.C., and Lee, W. Y., "Composite Development and Applications for Cryogenic Tankage," *Proceedings of the 46th AIAA/ASME/ASCE /AHS/ASC SDM Conference*, AIAA 2005-2160, Austin, TX, April, 2005.
2. Black, S., "An Update on Composite Tanks for Cryogenics," *High Performance Composites*, November, 2005, pp 22-27.
3. Gregnoble, R. W. and Gates, T. S., "Hydrogen Permeability of Polymer Matrix Composites at Cryogenic Temperatures," *Proceedings of the 46th AIAA/ASME/ASCE /AHS/ASC SDM Conference*, AIAA 2005-2086, Austin, TX, April, 2005.
4. Bechel, V. T., "Permeability and Damage in Unloaded Cryogenically Cycled PMCs," *Proceedings of the 46th AIAA/ASME/ASCE /AHS/ASC SDM Conference*, AIAA 2005-2156, Austin, TX, April, 2005.
5. Mallick, K., Cronin, J., Ryan, K., Arzberger, S., Munshi, N., Paul, C., and Welsh, J.S., "An Integrated Systematic Approach to Linerless Composite Tank Development," *Proceedings of the 46th AIAA/ASME/ASCE /AHS/ASC SDM Conference*, AIAA 2005-2089, Austin, TX, April, 2005.
6. Yokozeki, T., Aoki, T., and Ishikawa, T., "Gas Permeability of Laminates Under Cryogenic Conditions," *Proceedings of the 44th AIAA/ASME/ASCE /AHS/ASC SDM Conference*, AIAA 2003-1604, Norfolk, VA, April, 2003.
7. Bechel, V. T., Negilski, M., and James, J., "Limiting the Permeability of Composites for Cryogenic Applications," *Composites Science and Technology*, in press, available on line at www.sciencedirect.com, 2006.
8. Ju, J., Morgan, R.J., Shin, E.E., and Creasy, T.S., "Transverse Cracking of M40J/PMR-II-50 Composites under Thermal-Mechanical Loading: Part II – Experiment and Analytical Investigations," *Journal of Composite Materials*, in press, 2006.

9. Kim, R. Y., "Fatigue Behavior," *Composite Design*, edited by S.W. Tsai, Think Composites, Dayton, OH 1988, pp. 19-5 to 19-7.
10. Ju, J., Morgan, R.J., Shin, E.E., and Creasy, T.S., "Transverse Cracking of M40J/PMR-II-50 Composites under Thermal-Mechanical Loading: Part I – Characterization of Main and Interaction Effects Using Statistical Design of Experiments," *Journal of Composite Materials*, in press, 2006.



Figure 1: Cryogenic and elevated temperature thermal cycler



Figure 2: Permeability measurement apparatus

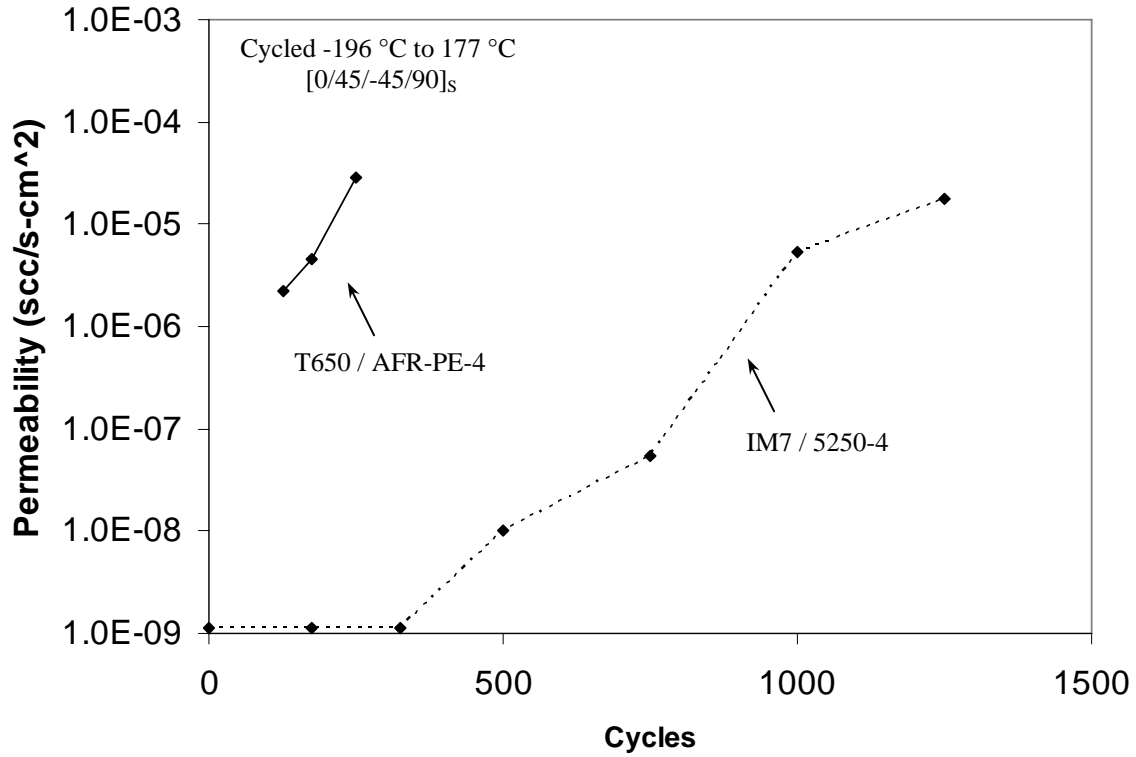


Figure 3: T650 / AFR-PE-4 and IM7 / 5250-4 [0/45/-45/90]_s permeability after -196 °C to 177 °C thermal cycling

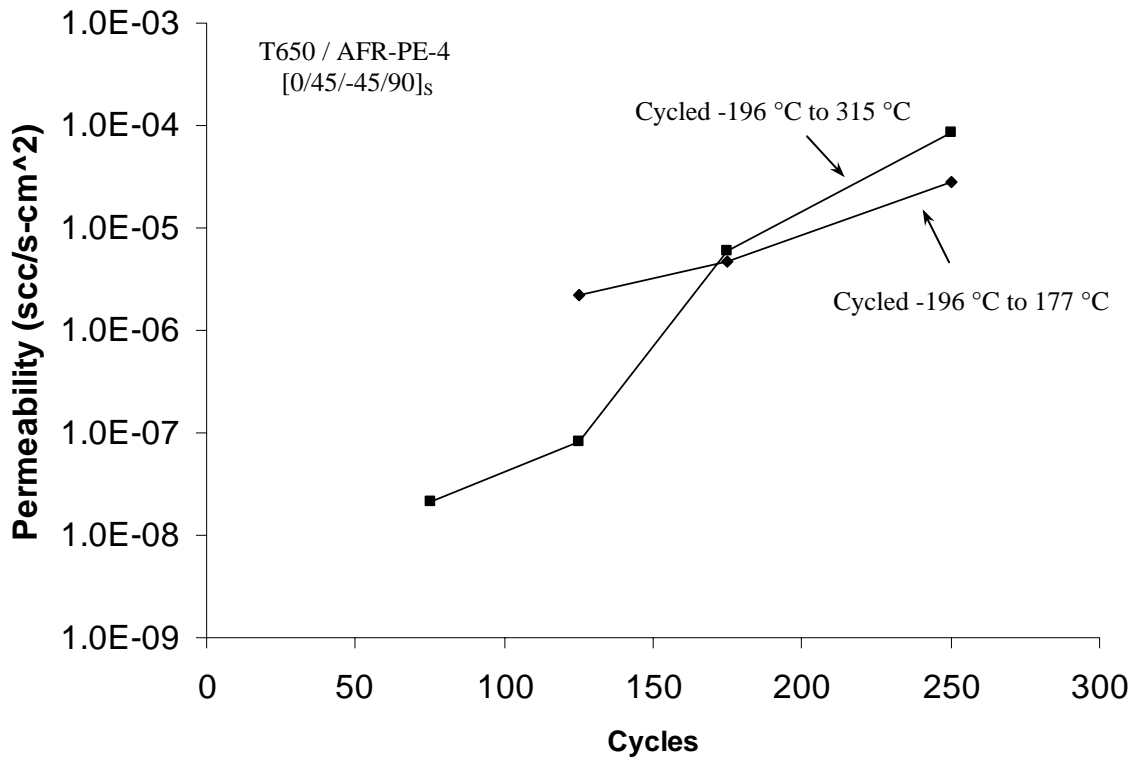


Figure 4: T650 / AFR-PE-4 [0/45/-45/90]_s permeability after -196 °C to 177 °C and -196 °C to 315 °C thermal cycling

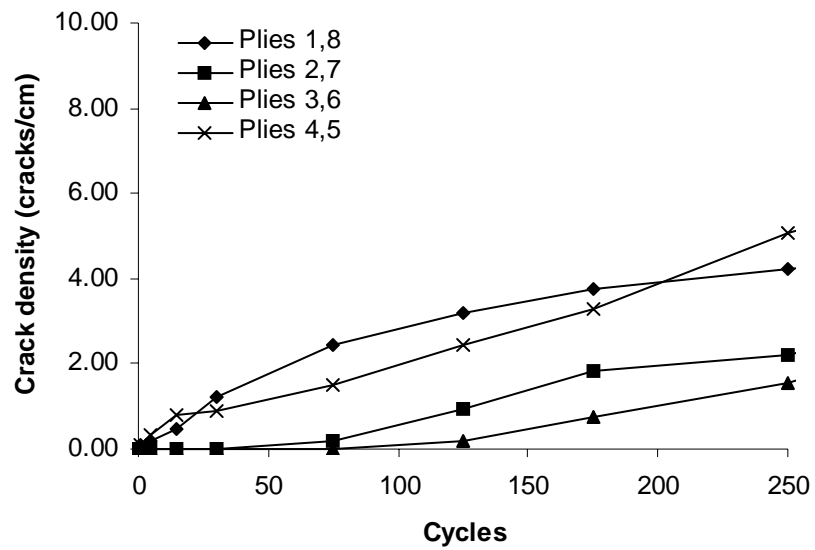


Figure 5: Damage in T650 / AFR-PE-4 [0/45/-45/90]_s as a function of -196 °C to 177 °C thermal cycling

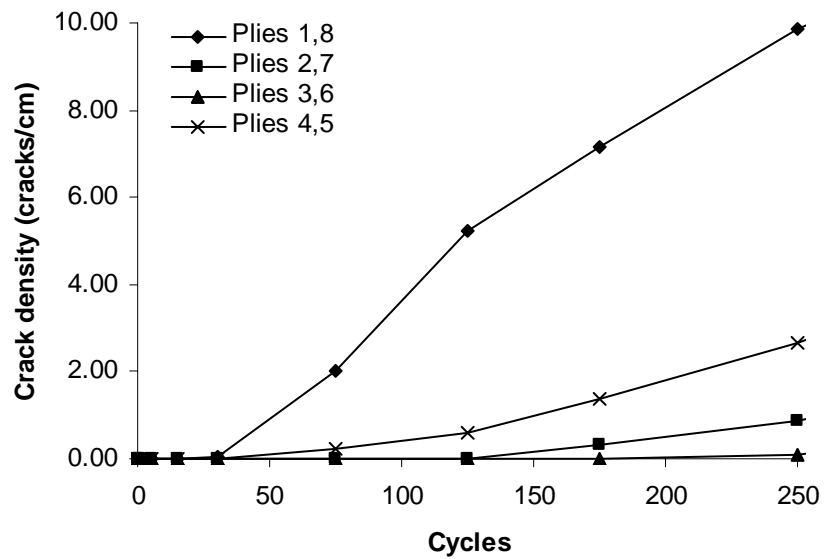


Figure 6: Damage in IM7 / 5250-4 [0/45/-45/90]_s as a function of -196 °C to 177 °C thermal cycling

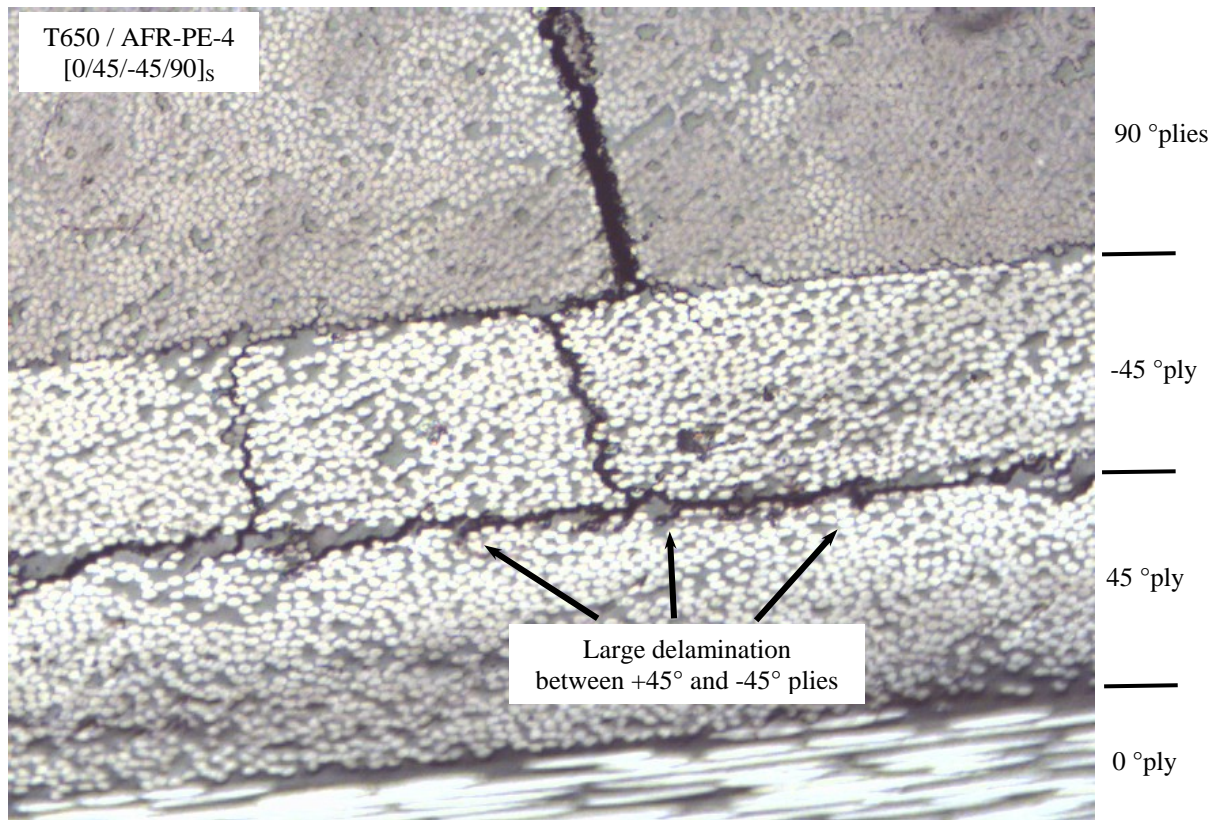


Figure 7: Image of damage in T650 / AFR-PE-4 after 250 cycles

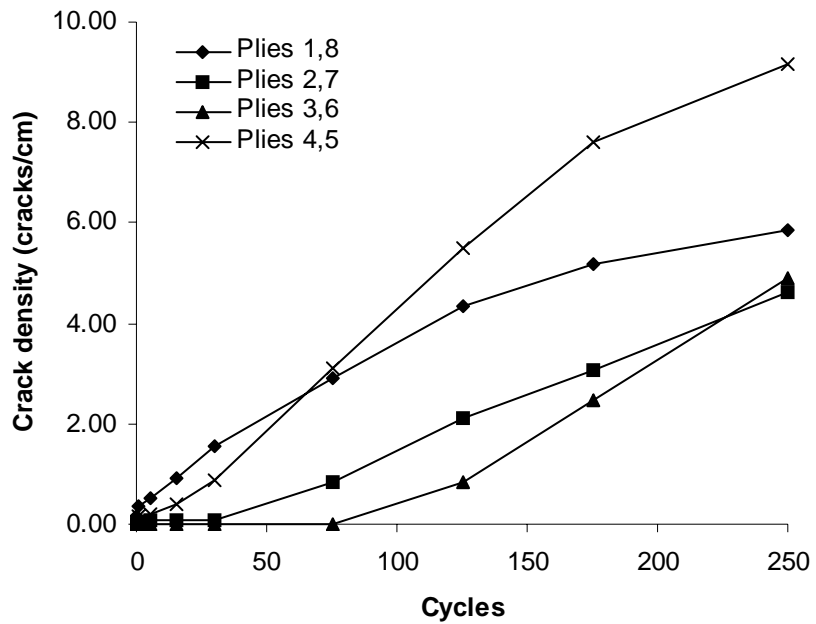


Figure 8: Damage in T650 / AFR-PE-4 [0/45/-45/90]_s as a function of -196 °C to 315 °C thermal cycling

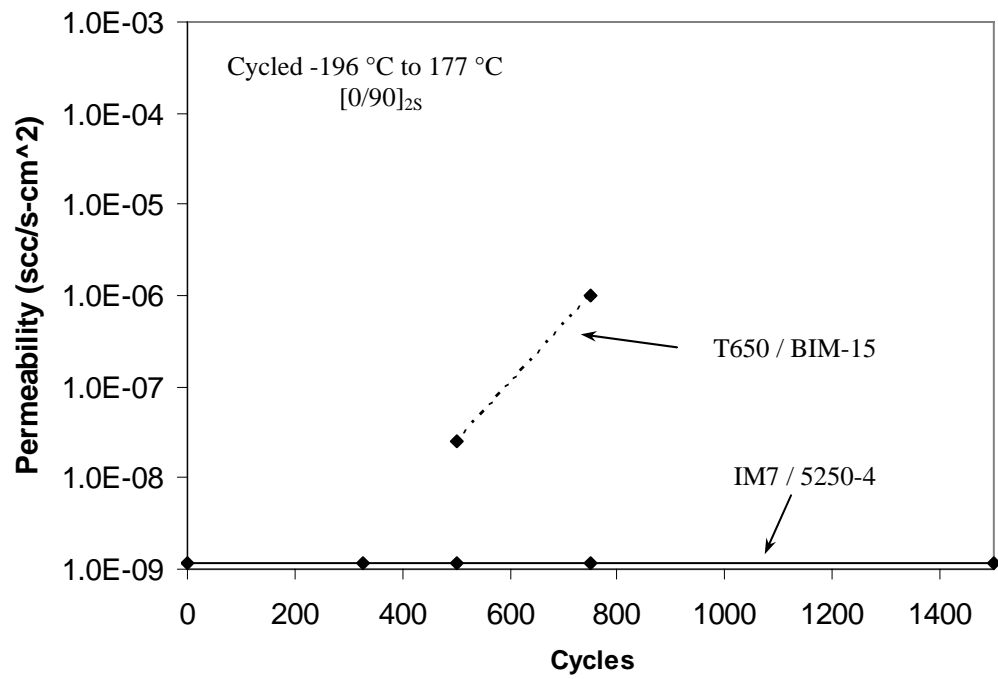


Figure 9: IM7 / 5250-4⁷ and T650 / BIM-15 [0/90]_{2s} permeability after -196 °C to 177 °C thermal cycling